Optical study of phonons and electronic excitations in tetragonal Sr_2VO_4

J. Teyssier,[1] R. Viennois,[1] E. Giannini,[1] R. M. Eremina,[2] A. Günther,[3] J. Deisenhofer,[3] M. V. Eremin,[4] and D. van der Marel[1]

[1]*Département de Physique de la Matière Condensée, Université de Genève, Quai Ernest-Ansermet 24, CH-1211 Genève 4, Switzerland*

[2]*E. K. Zavoisky Physical Technical Institute, 420029 Kazan, Russia*

[3]*Experimentalphysik V, Center for Electronic Correlations and Magnetism, Institute for Physics, Augsburg University, D-86135 Augsburg, Germany*

[4]*Kazan (Volga region) Federal University, 420008 Kazan, Russia*

(Received 6 October 2011; published 17 November 2011)

We report on the optical excitation spectra in Sr_2VO_4. The phonon modes are assigned and their evolution with temperature is discussed in the frame of the different phase transitions crossed upon cooling. Besides the expected infrared-active phonons, we observe two additional excitations at about 290 and 840 cm^{-1}, which could correspond to electronic transitions of the V^{4+} ions. Our experimental results are discussed in the context of recent experimental and theoretical studies of this material with a unique spin-orbital ground state.

DOI: 10.1103/PhysRevB.84.205130 PACS number(s): 78.20.Ls, 71.70.Ej, 75.25.Dk

I. INTRODUCTION

Sr_2VO_4 has the same layered crystal structure as the parent compound of the high T_c superconductors La_2CuO_4 (Refs. 1,2) and quasi-two-dimensional electronic behaviors. Both materials are Mott-Hubbard insulators, with one electron on the vanadium site in the case of Sr_2VO_4 and one hole per copper site for La_2CuO_4. Based on these similarities, several theoretical groups have suggested that doped Sr_2VO_4 could be superconducting.[3–5] The excruciating difficulty of synthesizing a polycrystalline powder of the pristine material gives less flexibility than in the cuprates to play with the stochiometry. While superconductivity has been elusive, Sr_2VO_4 passes as a function of temperature through a number of different electronic phases, which are not fully understood and which have not been observed in the cuprate family. Above 127 K, the material is paramagnetic. Below 97 K, the system enters a different magnetic and orbital state, which is not ferromagnetic, and the nature of which is the main subject of the present paper. A phase coexistence is found between 98 and 127 K.[6]

The most important difference in the electronic structure of La_2CuO_4 and Sr_2VO_4 results from the different ground-state degeneracy of the open $3d$ shell in both materials: The hole on the Cu atom in La_2CuO_4 occupies a $3d_{x^2-y^2}$ orbital. The single electron on the V ion in Sr_2VO_4 occupies the degenerate set of $3d_{xz}$ and $3d_{yz}$ orbitals. This orbital degree of freedom profoundly affects the physical properties, as we will see below.

Based on magnetic-susceptibility data, it was believed that the system undergoes an antiferromagnetic (AFM) transition with a sample-dependent Néel temperature ranging between 10 and 100 K, although no signs of long-range order could be found using neutron-scattering experiments.[1] Subsequent works reported a Néel temperature of 40 K (Ref. 7) and a strong dependence of the occurrence of these anomalies on the stoichiometry of the samples.[8] Only recently, it was shown that the system exhibits a phase transition at $T_1 \simeq 100$ K upon cooling, where the ratio of the tetragonal lattice parameters c/a increases abruptly while the magnetic susceptibility drops concomitantly.[6] Hence, the phase below T_1 was interpreted as antiferromagnetically and orbitally ordered.[6] Theoretical scenarios predict a stripelike orbital and collinear AFM spin ordering,[9] strong competition between ferromagnetism and antiferromagnetism,[9] or a magnetically hidden order of Kramers doublets due to the formation of *magnetic octupoles* mediated by spin-orbit coupling.[10] Recent inelastic neutron-scattering studies revealed a splitting of the highest-lying doublet of the V^{4+} ions persisting up to 400 K,[11] which indicates the presence of a finite dipolar magnetic moment and is difficult to reconcile with a purely octupolar magnetic order. We recently suggested that the system can be described in terms of an alternating spin-orbital order below the Néel temperature, and we derived the corresponding energy-level scheme for the V^{4+} ions.[12]

Here we investigate the low-energy optical excitation spectrum in tetragonal Sr_2VO_4. The phonon modes have been identified in the optical spectrum by comparison with the isomorphic compounds Sr_2TiO_4 (Refs. 13,14) and La_2NiO_4.[15] Their evolution upon cooling, i.e., crossing the different structural and (or) magnetic transitions, supports the scenario of a long-range orbital ordering. In addition to optical-phonon bands, we could identify two excitations. The first one is in the phonon-energy range (290 cm^{-1}) but does not correspond to any identified phonon. It shows a very strong temperature dependence at the temperature T_1 mentioned above. The second one (840 cm^{-1}) is too high to be a phonon and could correspond to the above-mentioned excitation observed by neutron scattering.[11] These two excitations correspond to excitation energies proposed in Ref. 12 as a result of the alternating spin-orbital ordered ground state.

II. SAMPLE PREPARATION AND EXPERIMENTAL DETAILS

Ceramic samples were synthesized from the reduction of homemade $Sr_4V_2O_9$ precursor using Zr as the reducing agent.[16] The reaction was done in a quartz tube under vacuum at 950 °C. The procedure was repeated several times with intermediate grinding. With this method, almost-single-phase tetragonal Sr_2VO_4 can be obtained. Lattice parameters were extracted from Rietveld refinements of the powder-diffraction pattern ($a = 3.8349$ Å, $c = 12.5646$ Å) and traces of the

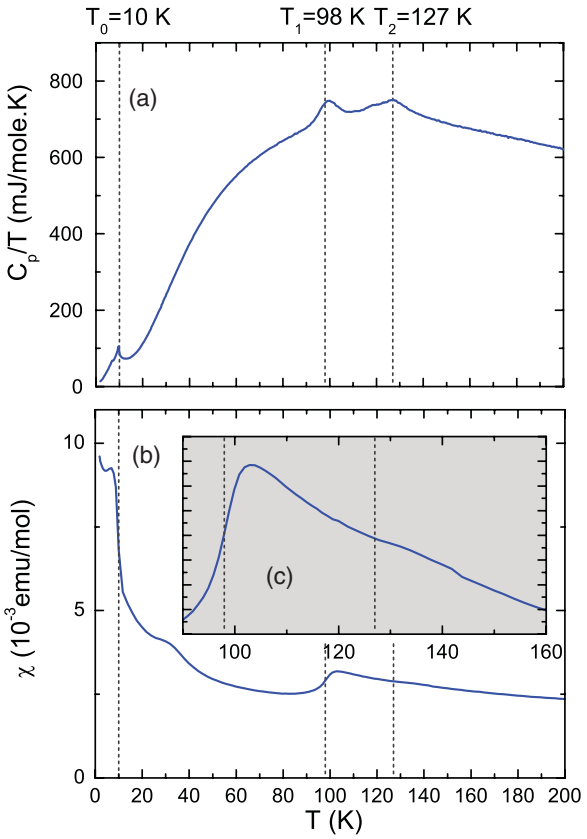

FIG. 1. (Color online) (a) Specific heat divided by temperature. (b) and (c) Magnetic susceptibility measured in 0.2 T.

orthorhombic phase of Sr_2VO_4 as well as $Sr_3V_2O_7$ were found within 3%.

The specific heat exhibits three peaks upon cooling [Fig. 1(a)]. A peak in the specific heat associated to a weak anomaly in the susceptibility at $T_2 = 127$ K [Fig. 1(b)] coincides with the reported onset of orbital order and a coexistence regime of the low- and high-temperature tetragonal phase for $T_1 \leqslant T \leqslant T_2$.[6] The sharp drop at $T_1 = 98$ K reveals the transition to the low-temperature tetragonal phase. A peak at 10 K indicates the transition to a phase with a weak ferromagnetic moment. Nozaki *et al.*[7] have measured a small hysteresis loop at 5 K with a ferromagnetic moment of about $10^{-4}\,\mu_B$, and a nonvanishing magnetic moment is also predicted by several theoretical studies.[3,9,17] A further broad anomaly, also visible at 35 K in the magnetic susceptibility, was reported earlier.[7] Since this feature varies rather strongly from one sample to another, it may not be an intrinsic property of tetragonal Sr_2VO_4. The peaks present in the magnetic susceptibility around 35 K could be attributed to $Sr_3V_2O_7$ as a secondary phase.[18] The Curie-like behavior of the magnetic susceptibility below the Néel temperature is very likely dominated by impurities.[12]

The reflectivity of the sample was measured in the infrared spectral range (12 meV and 0.8 eV) using a Fourier-transform spectrometer, and the complex dielectric function was measured in the range 0.8–4.5 eV using spectroscopic ellipsometry. For both measurements, the sample was mounted in a helium flow cryostat allowing measurements from room temperature down to 13 K. Absolute reflectivity was obtained by calibrating the signal against an *in situ* evaporated gold film on the sample surface.

III. EXPERIMENTAL RESULTS AND DISCUSSION

The experimental reflectivity is plotted in Fig. 2(a). The reflectivity, also measured in the far infrared in a magnetic field as high as 7 T, did not reveal any field dependence of the main features of the spectrum. The real and imaginary parts of $\epsilon(\omega)$ obtained using ellipsometry at selected temperatures are shown in Fig. 2(b). In order to obtain the optical conductivity over the full spectral range [Fig. 2(c)], we used a variational routine[19] yielding the Kramers-Kronig consistent dielectric function that reproduces all the fine details of the infrared reflectivity data, while *simultaneously* fitting to the complex dielectric function in the visible and UV range. This procedure anchors the phase of the infrared reflectivity to the phase at high energies. The temperature evolution of the optical conductivity in the visible

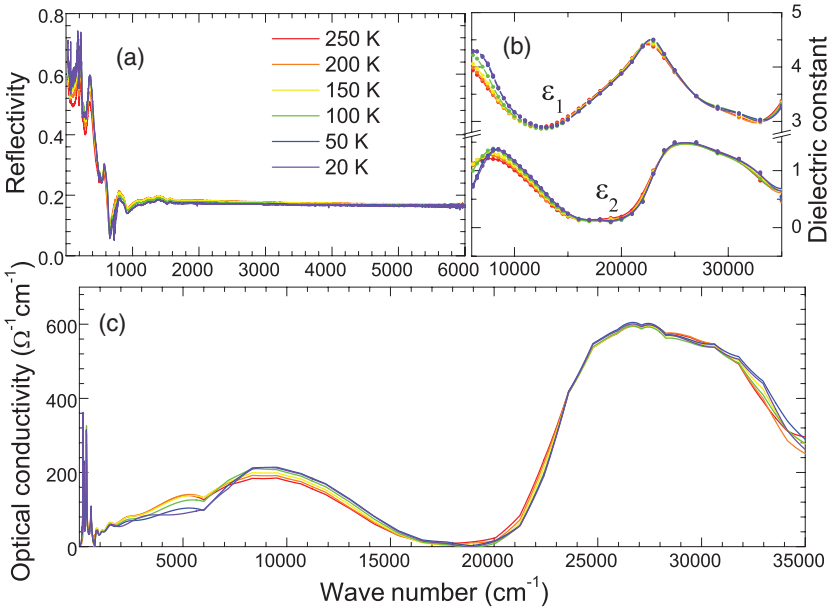

FIG. 2. (Color online) (a) Reflectivity measured in far and near infrared. (b) Real (ϵ_1) and imaginary (ϵ_2) part of the dielectric function measured by ellipsometry. (c) Real part of the optical conductivity (σ_1) for selected temperatures.

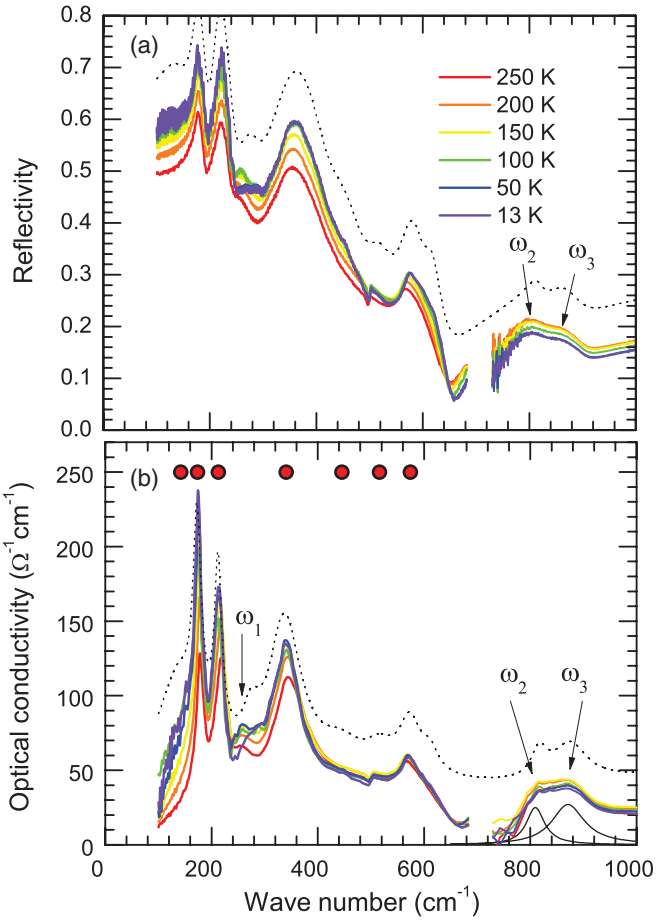

FIG. 3. (Color online) Low-energy part of the (a) reflectivity and (b) optical conductivity for different temperatures. The optical-phonon frequencies are indicated by filled circles. Interorbital optical excitations ω_1, ω_2, and ω_3 are marked by arrows. The dotted line corresponds to the Lorentz fit at 13 K (dotted curves were shifted for reasons of clarity).

range is in good agreement with previous measurements on epitaxial thin films.[20] Figure 3 shows the low-energy part of the reflectivity [panel (a)] and the corresponding optical conductivity [panel (b)]. The phonon modes that have been identified (see Sec. III A) are marked by solid dots.

A. Phonons

Tetragonal Sr_2VO_4 belongs to the D_{4h}^{17} symmetry group which has 7 infrared, 4 Raman, and 1 silent vibration mode. The assignment of the optical-phonon modes expected for the D_{4h}^{17} symmetry of Sr_2VO_4 has been made from a comparative study of vibration modes in the isostructural compounds Sr_2TiO_4 (Ref. 13) and La_2NiO_4.[15] Optical modes at 142, 174, 213, 340, 445, 516, 574, and 612 cm^{-1} (including some longitudinal components) are indicated by the filled circles in Fig. 3. Three additional optical excitations with eigenfrequencies ω_1, ω_2, and ω_3 do not have their counterpart in Sr_2TiO_4 and La_2NiO_4, and their origin will be discussed further. The temperature dependence of the phonon modes is shown as color maps of the optical conductivity in the left panels of Fig. 4.

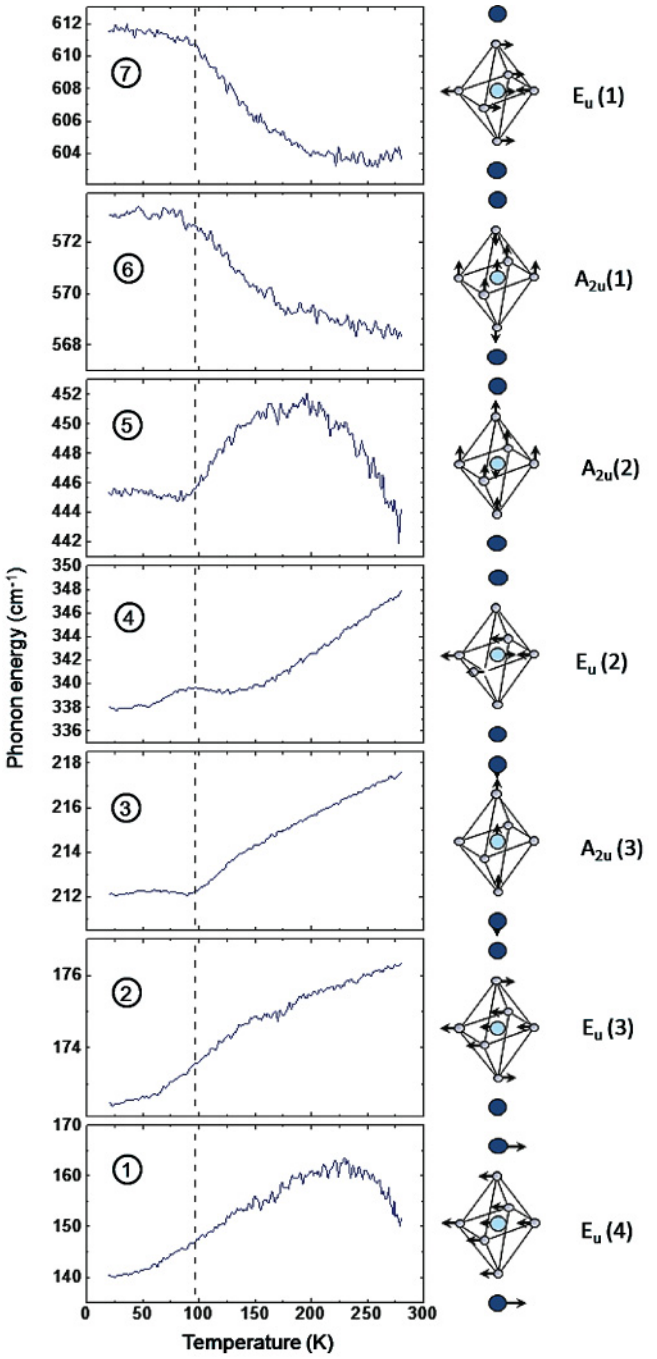

FIG. 4. (Color online) Left panels: Temperature dependence of the energy of phonon modes as numbered in Table I. Right panels: Associated ionic displacement and naming.

The parameters used to fit the phonon part of the optical data are given in Table I for three different temperatures.

From the Lorentz fit of the different modes, it is possible to follow the evolution of the central frequency upon cooling with a resolution of 1 K (Fig. 4). All phonon modes are sensitive to temperature in a different manner depending on the bonds involved and the anisotropy of thermal expansion. We have monitored the variation in the temperature trend of the mode frequency upon crossing the orbital-ordering transition. To disentangle the evolution of the phonon frequency due

TABLE I. Phonon fitting parameters of Sr_2VO_4 optical data at 280, 100, and 13 K. ω is the central frequency plotted in Fig. 4, Ω_p is the oscillator strength, and γ is the scattering rate of the Lorentz oscillator (units are cm^{-1}). $\Delta\frac{\partial\omega}{\partial T}$ represents the change in the slope of the phonon-energy temperature dependence at the orbital-ordering temperature, as defined in the text.

Mode No.	ϵ_∞		280 K 5.83			100 K 5.99			13 K 5.93			$\Delta\frac{\partial\omega}{\partial T}$ cm^{-1} K^{-1}	Error on $\Delta\frac{\partial\omega}{\partial T}$ cm^{-1} K^{-1}
	Mode	ω	Ω_p	γ	ω	Ω_p	γ	ω	Ω_p	γ		
1	$E_u(4)$	151	341	116	145	542	76	142	582	75	0.0769	0.1446
2	$E_u(3)$	179	298	19	175	418	18	174	427	18	−0.0119	0.0060
3	$A_{2u}(3)$	218	382	29	213	403	21	213	409	20	0.0478	0.0071
4	$E_u(2)$	349	702	92	341	714	74	340	719	75	−0.0660	0.0268
5	$A_{2u}(2)$	443	365	115	445	409	115	445	387	110	0.1449	0.0445
5′	$E_u(2)$LO	519	184	38	521	254	42	516	202	32	0.0020	0.0439
6	$A_{2u}(1)$	569	310	52	573	334	50	574	341	51	−0.0548	0.0212
7	$E_u(1)$	605	188	44	611	167	36	612	180	37	−0.0722	0.0224

to thermal expansion over the wide temperature range to the effect of orbital rearrangement, we have fitted the temperature dependence of the phonon frequency with a parabolic function above and below the transition temperature T_1. We define the change in slopes of the tangents of the two fits (above and below transition) at the temperature T_1 as

$$\Delta\frac{\partial\omega}{\partial T} = \frac{\partial\omega}{\partial T}\Big|_{T_1+\delta} - \frac{\partial\omega}{\partial T}\Big|_{T_1-\delta}. \quad (1)$$

Three different intervals for each fit are used to calculate error bars. We give in Table I the value of $\Delta\frac{\partial\omega}{\partial T}$ for all identified phonons. For the soft mode (1) and the mode 5′ [assigned to the longitudinal-optic (LO) mode], error bars on K are larger than the change in slope. For the remaining modes, we observe a hardening of vibrations 3 and 5 both involving z-axis displacement (A_{2u} modes) of the vanadium ion opposite to the four in-plane oxygen ions.

The $A_{2u}(1)$ mode (6) also involves displacement of the V ion along the z axis but in phase with the four in-plane oxygens, and thus is only slightly affected by the "in-plane hardening." In-plane modes (E_u modes) are softened by the transition. This supports a charge transfer from in-plane to the c-axis orbitals, which is the consequence of a long-range orbital ordering.

B. Discussion

The temperature dependence of the experimental optical conductivity associated with the excitation ω_1 (Fig. 5) is very different in terms of central frequency and spectral weight as compared to the "usual" temperature evolution of the phonons discussed above. Coming from high temperature, the eigenfrequency $\omega_1 = 254$ cm^{-1} (31.5 meV) remains almost constant and shifts to a slightly higher value of about 260 cm^{-1} in the phase-coexistence regime. Below about 80 K, ω_1 vanishes. When cooling below T_2, an additional mode with a frequency $\omega_1' = 290$ cm^{-1} (36 meV) emerges and persists down to the lowest temperatures. Note that the simultaneous observation of the two optical excitations in the temperature range of 80 K $\leqslant T \leqslant T_2$ coincides with the proposed coexistence of two distinct tetragonal phases.[6]

Given the known crystal structure of Sr_2VO_4, we exclude the possibility that ω_1, ω_2, and ω_3 are optical phonons, either from the material itself or from secondary phases that have been the object of a careful study of their own optical properties. The two peaks at $\omega_2 = 810$ and $\omega_3 = 870$ cm^{-1} are too high in energy to correspond to lattice vibrations. Moreover, they are close in energy to the twin peaks observed by inelastic neutron scattering at 115 and 125 meV.[11] With $\Delta E = 8$ meV, these excitations are the optical counterparts of the excitations reported by neutron scattering at about 120 meV with a splitting of about $\Delta E = 10$ meV. Energies differ by a factor of about 0.9. This is a natural consequence of the dispersion of the excitations, which for optical spectroscopy are around $k = 0$, whereas the aforementioned inelastic neutron spectra were integrated over k space.

The frequency of the ω_1 excitation is in good agreement with the calculated frequency (8.3 Thz $\simeq$ 277 cm^{-1}) of the silent B_{2u} mode.[15] This mode corresponds to vibration along the c axis of the four oxygen ions in the ab plane, in phase along the diagonals and with opposite phase along the edges

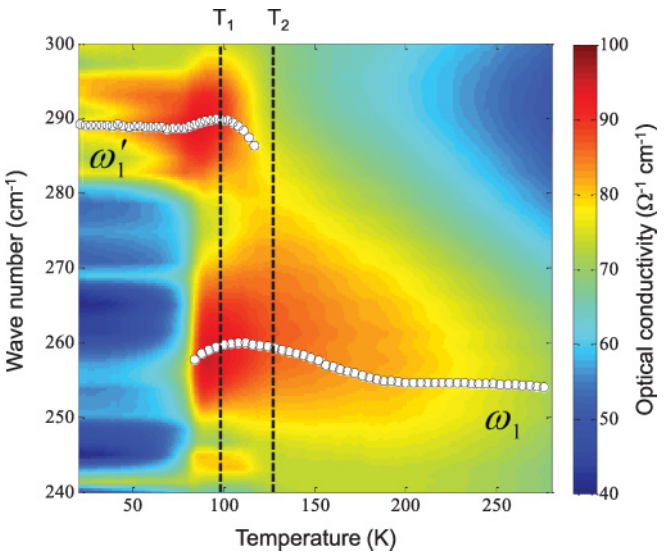

FIG. 5. (Color online) Color map of the experimental optical conductivity in the energy range corresponding to the low-energy set of transitions. The open symbols represent the temperature dependence of the central frequency of the Lorentz oscillator used to fit the reflectivity data. T_1 and T_2 correspond to the maxima of the two pronounced peaks in the specific heat.

of the ab oxygen square. The activation of this mode requires a breaking of the crystal symmetry that has so far not been observed in this material.

Another possibility could be that these three excitations are of an electronic origin. t_{2g} splits due to crystal field, spin-orbit coupling, and exchange fields. We compare our data to a microscopic model for the observed electronic excitation spectrum in Sr_2VO_4.[12] The relevant subset of the $3d$ crystal-field excitations is spanned by the t_{2g} levels, d_{xy}, d_{xz}, and d_{yz}. The tetragonal crystal-field splitting between d_{xz}/d_{xy} and d_{yz} is $3d$. The spin-orbit interaction $H_{SO} = \lambda \vec{L} \cdot \vec{S}$,[21] which in $d1$ systems tends to align spin and orbital angular momentum opposite to each other. The dominant exchange interaction with the surrounding V^{4+} ions in the ab plane is the antiferromagnetic superexchange J_a, between d_{xz} electrons on nearest-neighbor sites along the x axis, and likewise along the y axis. The second largest contribution is the ferromagnetic superexchange J_f, between d_{xy} and d_{yz} along the x axis, and likewise along the y axis. The ground state is formed by a Kramers doublet having orbital momentum $m_l = \pm 1$ ($\mu_l = 1 \cdot 1\mu_B$) and spin ($\mu_s = 2 \cdot \frac{1}{2}\mu_B$) pointing opposite to each other, causing an overall "mute" magnetic moment. Due to higher-order terms in the magnetic exchange interaction, the linear combination $u|d_{1,\downarrow}\rangle + v|d_{-1,\uparrow}\rangle$, with $u = cos(\eta/2)$ and $v = sin(\eta/2)$, has a weak dependence on η, as shown in Fig. 6. The magnetically most-stable state corresponds to $\eta = 0$.

The energy levels can be exactly calculated from the model and they are drawn as a function of the order parameter η in Fig. 6. The arrows represent the possible electronic transitions that could match with the ω_1, ω_2, and ω_3 transitions observed in the optical spectra.

By using the above level scheme for $\eta = 0$ (Fig. 6), we now obtain a consistent description of the observed optical excitation $\omega_1' = 290$ cm^{-1} ($\simeq$36 meV) and a double peak structure [Fig. 2(b)] with central frequencies of $\omega_2 = 810$ cm^{-1} (100 meV) and $\omega_3 = 870$ cm^{-1} (108 meV) at 20 K.

By using a value $\lambda \simeq -30$ meV equal to the free-ion value,[21] $J_a \simeq 15$ meV, $D = -33$ meV, and $J_f \simeq -9$ meV in the model described above, we get a good estimate for the excitation ω_1. The excitation pair $\omega_{2,3}$ between the lowest and the highest doublet is mainly determined by the crystal-field parameter, and the difference in energy $(\omega_3 - \omega_2)$ agrees with the splitting of 10 meV in the neutron-scattering spectra. The fact that this splitting reportedly persists up to 400 K indicates that short-range ordering is present in the system far above room temperature, and the level scheme should be valid even above the phase transition. We estimate that the reduction of D due to the reported reduced c/a ratio in the high-temperature tetragonal structure[6] is less than one percent. Therefore, we ascribe the energy difference of 4 meV of the optical excitation between the low- and high-temperature tetragonal structures and the decreasing splitting of the highest-lying levels to a somewhat smaller contribution of the spin-orbit interactions in the short-range ordered regime due to reduced intersite spin-spin correlations.

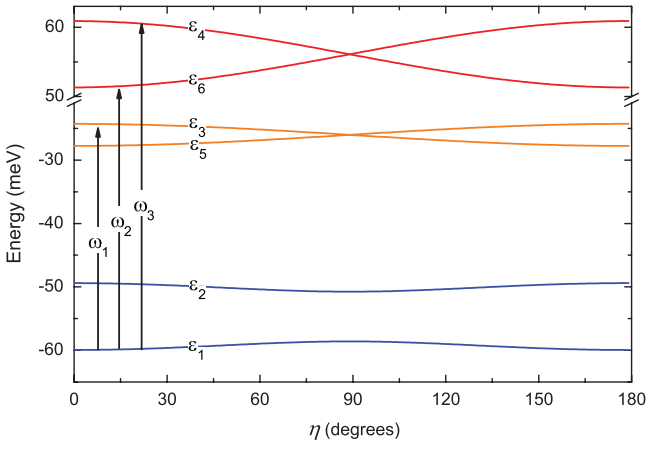

FIG. 6. (Color online) η dependence of electron level splitting due to the effects of the tetragonal crystal field, spin-orbit interaction, and antiferromagnetic and ferromagnetic superexchange. Optical transitions are indicated as arrows.

Having consistently described the observed optical excitations using this model, the remaining question is why these excitations are optically active. Given the symmetries of the Sr_2VO_4 as they have been described in the literature, and as we have assumed them to be in our discussion, the ground state and the excited states within the t_{2g}^1 manifold all have even parity. Consequently, under this assumption, none of the three excitations discussed above are expected to be electric-dipole active. Instead, since they are of the magnetic-dipole variety, we expect a relatively small oscillator strength.[22,23] For an isolated ion with $\eta = 0$, the selection rule $\Delta J_z = \pm 1$ applies to the optical transitions at ω_1 and ω_3. The excitation at ω_2 requires $\Delta J_z = 2$, which corresponds to a quadrupole transition. The admixture of $|d_{1,\downarrow}\rangle$ and $|d_{-1,\uparrow}\rangle$ in the ground state gives a dipole such as $\Delta J_z = \pm 1$ for the excitation ω_2. An alternative possibility is a mechanism described by Tanabe *et al.*,[24] whereby a finite electric-dipole matrix element is induced by the breaking of inversion symmetry of a *pair* of neighboring spins, as observed in FeF_2.[25]

IV. CONCLUSIONS

We have measured the infrared and visible optical spectrum of tetragonal Sr_2VO_4 at low temperature. In addition to well-identified phonon bands, an additional peak was observed, the origin of which could be

(i) a nonoptically active phonon that is made ir active due to breaking of the crystal-field symmetry, or

(ii) the electronic excitation spectrum of the V^{4+} ions that supports a scenario of a novel ordered state in terms of an alternating spin-orbital order in Sr_2VO_4.

In this last scenario, the magnetic moments are muted by spin-orbit interaction. At low temperature, these muted moments are antiferromagnetically ordered. At elevated temperatures, the long-range order is lost, resulting in a high-temperature phase, which is again tetragonal. Since the ordering involves not only spin, but also orients the angular moments of the ions, the resulting magnetostriction should be particularly strong. This is probably the reason for the change of the lattice constant when the system orders and for the coexistence of two thermodynamically distinct phases in a certain temperature range.

ACKNOWLEDGMENTS

We gratefully acknowledge D. I. Khomskii and G. Jackeli for helpful and stimulating discussions. This work is supported by the SNSF through Grant No. 200020-130052 and the National Center of Competence in Research (NCCR) "Materials with Novel Electronic Properties-MaNEP." We acknowledge partial support by the DFG via the Collaborative Research Center TRR 80. M.V.E. is partially supported by the Ministry of Education of the Russian Federation via Grant No. 1.83.11.

[1] M. Cyrot, B. Lambertandron, J. Soubeyroux, M. Rey, P. Dehauht, F. Cyrot-Lackmann, G. Fourcaudot, J. Beille, and J. Tholence, J. Solid State Chem. **85**, 321 (1990).

[2] M. J. Rey, P. Dehaudt, J. C. Joubert, B. Lambert-Andron, M. Cyrot, and F. Cyrot-Lackmann, J. Solid State Chem. **86**, 101 (1990).

[3] W. Pickett, D. Singh, D. Papaconstantopoulos, H. Krakauer, M. Cyrot, and F. Cyrot-Lackmann, Physica C **162-164**, 1433 (1989).

[4] D. Singh, D. Papanconstantopoulos, H. Krakauer, B. Klein, and W. Pickett, Physica C **175**, 329 (1991).

[5] R. Arita, A. Yamasaki, K. Held, J. Matsuno, and K. Kuroki, J. Phys. Condens. Matter **19**, 365204 (2007).

[6] H. D. Zhou, B. S. Conner, L. Balicas, and C. R. Wiebe, Phys. Rev. Lett. **99**, 136403 (2007).

[7] A. Nozaki, H. Yoshikawa, T. Wada, H. Yamauchi, and S. Tanaka, Phys. Rev. B **43**, 181 (1991).

[8] N. Suzuki, T. Noritake, and T. Hioki, Mater. Res. Bull. **27**, 1171 (1992).

[9] Y. Imai, I. Solovyev, and M. Imada, Phys. Rev. Lett. **95**, 176405 (2005).

[10] G. Jackeli and G. Khaliullin, Phys. Rev. Lett. **103**, 067205 (2009).

[11] H. D. Zhou, Y. J. Jo, J. Fiore Carpino, G. J. Munoz, C. R. Wiebe, J. G. Cheng, F. Rivadulla, and D. T. Adroja, Phys. Rev. B **81**, 212401 (2010).

[12] M. V. Eremin, J. Deisenhofer, R. M. Eremina, J. Teyssier, D. van der Marel, and A. Loidl, e-print arXiv:1111.0668 (unpublished); J. Deisenhofer *et al*. (in preparation).

[13] G. Burns, F. H. Dacol, G. Kliche, W. Konig, and M. W. Shafer, Phys. Rev. B **37**, 3381 (1988).

[14] C. J. Fennie and K. M. Rabe, Phys. Rev. B **68**, 184111 (2003).

[15] L. Pintschovius, J. M. Bassat, P. Odier, F. Gervais, G. Chevrier, W. Reichardt, and F. Gompf, Phys. Rev. B **40**, 2229 (1989).

[16] R. Viennois, E. Giannini, J. Teyssier, J. Elia, J. Deisenhofer, and D. van der Marel, J. Phys. Conf. Ser. **200**, 012219 (2010).

[17] R. Arita, A. Yamasaki, K. Held, J. Matsuno, and K. Kuroki, Phys. Rev. B **75**, 174521 (2007).

[18] R. Fukushima, and A. Ando, Phase Transit. **41**, 149 (1993).

[19] A. B. Kuzmenko, Rev. Sci. Instrum. **76**, 83108 (2005).

[20] J. Matsuno, Y. Okimoto, M. Kawasaki, and Y. Tokura, Phys. Rev. Lett. **95**, 176404 (2005).

[21] A. Abragam and B. Bleaney, *Electron Paramagnetic Resonance of Transition Ions* (Oxford University Press, Oxford, 1970).

[22] Ch. Kant, T. Rudolf, F. Schrettle, F. Mayr, J. Deisenhofer, P. Lunkenheimer, M. V. Eremin, and A. Loidl, Phys. Rev. B **78**, 245103 (2008).

[23] S. Sugano, Y. Tanabe, and H. Kamimura, *Multiplets of Transition-Metal Ions in Crystals* (Elsevier, New York, 1970).

[24] Y. Tanabe, T. Moriya, and S. Sugano, Phys. Rev. Lett. **15**, 1023 (1965).

[25] J. W. Halley and I. Silvera, Phys. Rev. Lett. **15**, 654 (1965).